Freeze tolerance influenced forest cover and hydrology during the Pennsylvanian

William J. Matthaeus[a,1], Sophia I. Macarewich[b], Jon D. Richey[a], Jonathan P. Wilson[c], Jennifer C. McElwain[d], Isabel P. Montañez[e], William A. DiMichele[f], Michael T. Hren[g], Christopher J. Poulsen[b], and Joseph D. White[a]

[a]Department of Biology, Baylor University, Waco, TX 76706; [b]Earth and Environmental Sciences, University of Michigan, Ann Arbor, MI 48109; [c]Department of Environmental Studies, Haverford College, Haverford, PA 19041; [d]Botany, Trinity College Dublin, Dublin 2, Ireland D02 PN40; [e]Department of Earth and Planetary Sciences, University of California, Davis, CA 95616; [f]Department of Paleobiology, Smithsonian Institution, Washington, DC 20560; and [g]Department of Geosciences, University of Connecticut, Storrs, CT 06269

Edited by Anna K. Behrensmeyer, Smithsonian National Museum of Natural History, Washington, DC, and approved August 16, 2021 (received for review December 24, 2020)

The distribution of forest cover alters Earth surface mass and energy exchange and is controlled by physiology, which determines plant environmental limits. Ancient plant physiology, therefore, likely affected vegetation-climate feedbacks. We combine climate modeling and ecosystem-process modeling to simulate arboreal vegetation in the late Paleozoic ice age. Using GENESIS V3 global climate model simulations, varying pCO_2, pO_2, and ice extent for the Pennsylvanian, and fossil-derived leaf C:N, maximum stomatal conductance, and specific conductivity for several major Carboniferous plant groups, we simulated global ecosystem processes at a 2° resolution with *Paleo*-BGC. Based on leaf water constraints, Pangaea could have supported widespread arboreal plant growth and forest cover. However, these models do not account for the impacts of freezing on plants. According to our interpretation, freezing would have affected plants in 59% of unglaciated land during peak glacial periods and 73% during interglacials, when more high-latitude land was unglaciated. Comparing forest cover, minimum temperatures, and paleo-locations of Pennsylvanian-aged plant fossils from the Paleobiology Database supports restriction of forest extent due to freezing. Many genera were limited to unglaciated land where temperatures remained above −4 °C. Freeze-intolerance of Pennsylvanian arboreal vegetation had the potential to alter surface runoff, silicate weathering, CO_2 levels, and climate forcing. As a bounding case, we assume total plant mortality at −4 °C and estimate that contracting forest cover increased net global surface runoff by up to 6.1%. Repeated freezing likely influenced freeze- and drought-tolerance evolution in lineages like the coniferophytes, which became increasingly dominant in the Permian and early Mesozoic.

modeling | carboniferous | freezing | forest cover | runoff

Glacial–interglacial cycles during Earth's penultimate icehouse, the late Paleozoic ice age [LPIA; 340 to 285 Ma (1, 2)], subjected plants to oscillating, contrasting stressors. These stressors resulted in repeated vascular-plant community turnovers (2–4). Plant water use has been discussed as the causal link between climate and community change (2–5). Nevertheless, the freezing of internal plant water is an equally important dimension of water-related stress, particularly as plants exploited more terrestrial environments (6–8). The LPIA is characterized by high pO_2, fluctuating atmospheric pCO_2, and low solar luminosity (9). The continental arrangement and paleotopography were also unlike those of today. The Pangaean supercontinent had large areas of southern high-latitude land and an equatorial Central Pangaean Mountainous Region (CPMR) of varying topographic relief. Each of these phenomena produced sustained low temperatures that characterized large tracts of the Earth's surface (Fig. 1 and *SI Appendix*). Due to stresses like low temperature, the LPIA is likely important in the evolutionary history of vascular plants.

Periods of low temperature constrict forested areas, for example, during the Last Glacial Maximum compared to the preindustrial Holocene (10). Freezing temperatures likely limited the survivorship of arboreal plants during the LPIA. Furthermore, much of Gondwanaland, the southern half of supercontinent Pangaea, was not available for arboreal plants during peak glacial periods due to land ice cover (Fig. 1). Still, there is macrofossil evidence for abundant, diverse, and widespread terrestrial plant ecosystems on the supercontinent Pangaea (2, 11, 12). Plants that evolved some freeze tolerance before or during the LPIA would have colonized higher latitudes and elevations and influenced evolution and surface processes. However, the environmental limitations of plant physiology—for example, which arboreal plants were tolerant of freezing—and the extent of forest cover in Paleozoic Earth are not well understood.

The extent of Paleozoic plant distribution has been inferred from the fossil record (13). Paleozoic climate characteristics have also been used to infer Paleozoic phytogeography based on assumed functional equivalencies between contemporary and Paleozoic plants (14). Paleozoic climate can be estimated using global climate models (GCMs) modified to incorporate past environmental conditions [e.g., atmospheric CO_2 and O_2 levels, paleogeography, and glacial ice extent (15)]. Assumed functional equivalencies between contemporary and Paleozoic plants are a common and valuable strategy. However, this may limit the

Significance

Computer-assisted studies of natural history that consider extinct plant function contribute to the understanding of how Paleozoic glacial cycles controlled the distribution of forest cover and continental surface erosion. Simulated plant water balance supports widespread vegetation during the late Paleozoic ice age (LPIA). However, physiological inference suggests that plant freezing limited the geographic distribution of vegetation. Assuming LPIA plants had limited freeze tolerance, we found that increased surface runoff could have contributed to late Paleozoic climate change. Modeling that combines deep time climate reconstructions and paleobotanical data improves understanding of past Earth systems, which can help project future change.

Author contributions: W.J.M. and J.D.W. designed research; W.J.M., S.I.M., J.D.R., J.P.W., J.C.M., I.P.M., W.A.D., M.T.H., C.J.P., and J.D.W. performed research; W.J.M., S.I.M., J.D.R., I.P.M., and J.D.W. analyzed data; and W.J.M., S.I.M., J.D.R., J.P.W., J.C.M., I.P.M., W.A.D., M.T.H., C.J.P., and J.D.W. wrote the paper.

The authors declare no competing interest.

This article is a PNAS Direct Submission.

See online for related content such as Commentaries.

[1]To whom correspondence may be addressed. Email: will_matthaeus@baylor.edu.

This article contains supporting information online at https://www.pnas.org/lookup/suppl/doi:10.1073/pnas.2025227118/-/DCSupplemental.

Published October 11, 2021.

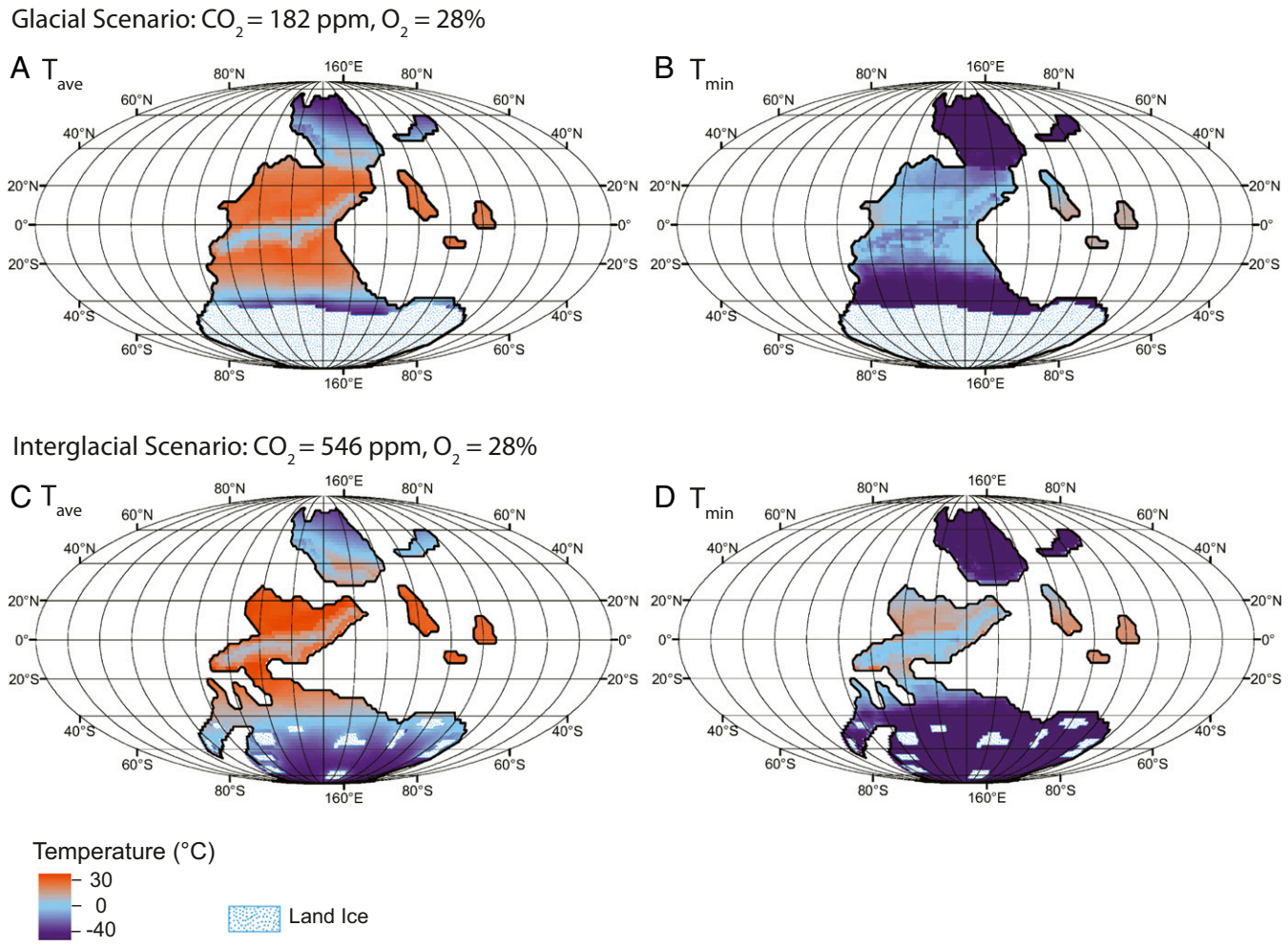

Fig. 1. Maps of average (T_{ave}: *A* and *C*) and daily minimum near-surface temperature (T_{min}: *B* and *D*) from a general circulation model (GENESIS V3) for the Pennsylvanian at 2-degree (longitude, latitude) resolution. Maps are in the Molleweide projection. The top maps (*A* and *B*) are from the glacial scenario with 182 ppm atmospheric CO_2 and 28% O_2. The bottom maps (*C* and *D*) are from the interglacial scenario with 546 ppm atmospheric CO_2 and 28% O_2. Ocean and glaciated areas are shown as white. Average temperature conditions were favorable in many locations (*SI Appendix*) where freezing minimum temperatures had the potential to limit plant growth.

accuracy of phytogeographic predictions because significant morphological or anatomical differences between many Paleozoic taxa and contemporary counterparts (e.g., nearest living relative [NLR]) suggest functional differences. Carboniferous lycopsids and sphenophytes, for example, were much larger than their NLR. Other Paleozoic plants have no NLR for comparison (e.g., pteridosperms). Paleozoic plant functional traits have been derived from measurements of fossil leaf cuticles, stems, and roots (16–23). These fossil-derived plant functional traits, along with regional GCM climate data, have been used to model Paleozoic ecosystem processes, including gas exchange, photosynthetic rates, and plant productivity (2, 24, 25). By combining global GCM data with fossil-derived ecosystem process modeling, we refine previous projections of forest cover during the LPIA (2, 5).

We simulate global ecosystem processes using *Paleo*-BGC (24) for the Pennsylvanian period utilizing daily output from the GENESIS V3 GCM (26, 27) (*Materials and Methods* and *SI Appendix*, Fig. S1). Our two parallel analyses are based on a simulation set for each extreme of LPIA glacial glacial–interglacial cycles, which varied in step with fluctuating pCO_2 and eccentricity (23). We parameterized *Paleo*-BGC using plant-fossil–derived foliar measurements of arborescent lycophytes (lycopsids), sphenophytes, pteridosperms, stem-group marattialean tree ferns, and early-diverging coniferophytes (cordaitaleans) from the Carboniferous (see ref. 2 for discussion of these plant types). We use leaf area index [LAI; m^2 leaf · m^{-2} ground (28)] from *Paleo*-BGC as a key model output due to its importance to plant gas exchange, productivity, and site water balance. LAI is presented here as a proxy for forest cover (*Study Caveats*). *Paleo*-BGC LAI maps for glacial and interglacial scenarios are limited only by carbon and water balance. As such, we present these maps as a maximum extent of forest cover distribution for each climate scenario, subject to further refinement. Actual forest cover was likely subject to other limiting factors, including mortality of plants due to freezing, which *Paleo*-BGC does not simulate.

Freezing minimum temperatures are crucial for predicting plant survivorship (e.g., US Department of Agriculture Plant Hardiness Zones). A single night of low temperature may induce freeze mortality with catastrophic consequences for vegetation communities (29). In addition to general Paleozoic climate characteristics, GCMs provide information on the frequency and severity of extreme events, such as minimum temperatures, that are not captured by monthly to annual climatologies (e.g., mean annual temperature). We compare our simulated forest vegetation

cover and the distribution of fossil occurrences of vascular plants from the Paleobiology Database (PBDB) to GCM-derived minimum temperature extremes. This comparison serves to 1) further constrain *Paleo*-BGC predictions of plant growth based only on carbon and water budgets and 2) provide a framework for future investigation of freeze tolerance evolution in LPIA plant taxa.

Finally, based on the synthesis of physiology, modeling, and fossil data, we present a case study that demonstrates the potential scale of the effect of reduced vegetation cover on hydrology. To facilitate this study, we assume only minimal freeze tolerance had evolved in the Paleozoic vegetation, specifically, that minimum temperatures below −4 °C resulted in total plant mortality. This limitation of plants corresponds to an estimated minimum extent of the distribution of forest cover. We then estimate the change in surface runoff resulting from our assumed limitation of forest cover by freezing. Depending on the coincidence of freeze-intolerant plants, lithology, paleotopography, and other factors, vegetative changes due to freezing may have altered terrigenous material transport and silicate weathering and thus the degree of weatherability and coupling between CO_2 and climate during the late Paleozoic (30–32).

Results

Our simulations predict global average 10-y minimum daily temperatures of −22.9 °C (±23.7, 1 SD; CO_2 = 182 ppm) in the glacial scenario and −29.0 °C (±28.0, 1 SD; CO_2 = 546 ppm) in the interglacial scenario. In the glacial scenario, 70% of the land surface was unglaciated, whereas 95% of the interglacial scenario land surface was unglaciated (*Materials and Methods* and *Study Caveats*). Glacial temperature averages were higher than interglacial temperature averages for ice-free land because of the sizeable, glaciated area in the southern hemisphere of the glacial scenario (Fig. 1 *A* and *B* and *SI Appendix*). Most locations, including many low latitude locations, had freezing minimum temperatures in the glacial scenario (Fig. 1*B*). Across tropical terrestrial locations, the average minimum temperature was 12.6 °C (±10.2) in the glacial scenario and 19.5 °C (±6.5) in the interglacial scenario. Nonfreezing locations in the glacial scenario were located in the coastal and paramontane tropics and the Cathaysian Islands. In the interglacial scenario, freezing minimum temperatures were ubiquitous at greater than 25° latitude and occurred sporadically in low-latitude, high-altitude locations (Fig. 1*D*).

Ecosystem process simulations (*Paleo*-BGC) were run on all ice-free terrestrial locations. The overall mean LAI for the Pennsylvanian was 3.3 (±4.4). In the glacial scenario (CO_2 = 182 ppm), global mean LAI was 2.3 (±2.9), which was 55% of mean LAI in the interglacial scenario (CO_2 = 546 ppm) with a value of 4.2 (±2.7). Simulated LAI grouped by Köppen climate classification (33) compared favorably to field-measured LAI across modern forest biomes associated with the same climates (28, 34) (Table 1, *Discussion*, *Study Caveats*, and *SI Appendix*).

Locations that supported simulated arboreal vegetation cover (average LAI ≥ 0.1; *Materials and Methods*) in the glacial scenario were at low latitudes and midlatitudes, with intervening areas of minimal LAI (Fig. 2*A*).

In the interglacial case, locations supporting arboreal vegetation were nearly global, except for a few locations at latitudes > 50° (Fig. 2*B*). The paleo-locations of Pennsylvanian plant fossil occurrences from the PBDB (paleobiodb.org) were within areas that could support arboreal vegetation based on *Paleo*-BGC predictions. However, the distribution of fossil occurrences did not reflect the extent of forest cover predicted by *Paleo*-BGC. There were very few fossil occurrences recorded in the PBDB from outside of the paleo-tropics (i.e., South America, Africa, or Australia; Fig. 2). While plant communities growing outside tropical regions during the late Carboniferous have been assumed to be less abundant and diverse (35), preservation, collection, and other biases likely reduced their representation in the fossil record.

Table 1. Comparison of LAI from field measurements of modern forest biomes (28, 102) and Paleo-BGC simulated LAI for Pennsylvanian glacial and interglacial extremes by climate zone

	Modern field measured LAI			Pennsylvanian Paleo-BGC simulated LAI							
				Glacial				Interglacial			
Bioclimatic zone	Mean	Min	Max	Mean	SD	Min	Max	Mean	SD	Min	Max
Tropical	7.4	4.2	12.4	8.4	1.9	2.8	13.0	11.3	1.3	9.0	15.3
Montane Tropical	4.6	0.6	8.9	2.8	2.9	0.1	6.5	5.0	2.7	0.7	12.6
Temperate	5.4	0.1	15.0	4.2	1.9	0.2	10.4	8.2	2.7	2	15.2
Boreal	2.7	0.5	6.2	2.1	1.3	<0.1	6.7	3.3	1.7	<0.1	10.3
Polar	1.9	0.2	5.3	1.1	0.9	<0.1	5.3	1.1	1.0	<0.1	8.7

Simulation grid cells are classified into Köppen climatic zones (A = tropical, C = temperate, D = boreal/continental, E = polar/alpine). In addition, Köppen zone E is divided into tropical, montane, and polar groups. See *SI Appendix* for details.

Overlaying the GENESIS V3 minimum temperature data (T_{min}) with forest vegetation cover simulated with *Paleo*-BGC (*SI Appendix*, Fig. S1) revealed that much of the unglaciated land that was predicted to support vegetation based on water balance was also affected by freezing temperatures. In the glacial scenario, 59% of unglaciated land area that supported vegetation also froze (Table 2; cumulative up to $T_{min} \leq 0$ °C). Large high-latitude areas were unglaciated in the interglacial scenario, allowing 73% of unglaciated land to be both vegetated and freezing. When we overlaid glacial scenario GENESIS V3 data on PBDB fossil paleo-locations, many plant fossil occurrences were in freezing locations (Table 2, Fig. 2, *SI Appendix*). Most fossil occurrences were in locations where $T_{min} > -40$ °C, however, and only a few genera were found in colder areas (*SI Appendix*, Fig. S9). For the interglacial, GENESIS V3 predicted that the same paleo-locations were warmer, with most fossil occurrences in locations with $T_{min} > -4$ °C (note that fossil locations were not partitioned into glacial and interglacial; see *Study Caveats*). However, for both glacial and interglacial scenarios, seed-bearing plant (i.e., spermatophyte) lineage groups and sphenophytes occurred in locations with $T_{min} > -40$ °C (Table 2).

Discussion

Our ecosystem simulations provide preliminary process-based estimates of the global extent of forest cover for the Pennsylvanian (323 to 299 Ma). We do not explicitly model non-arborescent plants. However, in locations where water was available but freezing limited arboreal forms, freeze-tolerant herbaceous tracheophytes, basal embryophytes, and lichens may have persisted (36). These data further confirm that global conditions allowed widespread vegetation across the Pangaean supercontinent, particularly during warmer interglacial periods of the Pennsylvanian (Figs. 1 and 2 and Table 2). While simulated LAI compares favorably to field-measured LAI across Köppen climate classifications (33) (Table 1, *Study Caveats*, *SI Appendix*), *Paleo*-BGC relies on C:*N*-based estimates of specific leaf area (SLA) values for extinct plants to convert modeled leaf mass to projected LAI (24). In the future, we suggest that these estimates could be improved using alternative proxies for leaf mass, such as the petiole width (37), adaxial epidermal density (38), and cuticle thickness (39). Furthermore, forests were likely

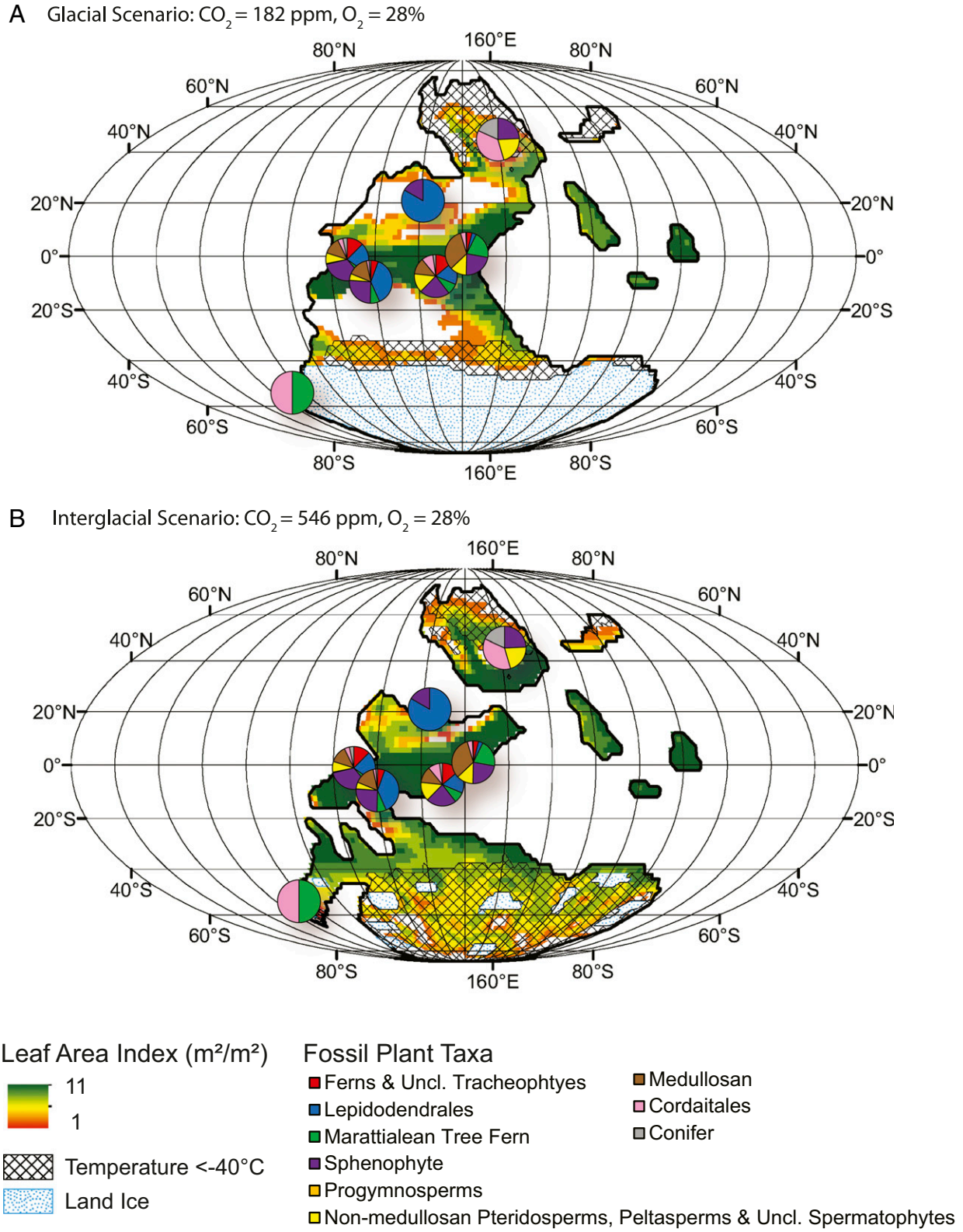

Fig. 2. Maps of LAI in the Pennsylvanian in the Molleweide projection. A general circulation model (GENESIS V3) was used to produce global daily data (T_{min}, T_{max}, precipitation; *Materials and Methods*) at 2-degree (longitude, latitude) resolution. These data were used as inputs to an ecosystem process model (*Paleo*-BGC) that was parameterized using measurements from leaf fossils to simulate LAI. Each map is a mosaic of simulations representing the mean LAI produced by eight representative Pennsylvanian taxa under each scenario. LAI maps are overlaid with pie charts representing locations of Pennsylvanian fossil occurrences from the PBDB (http://paleobiodb.org). Based on water balance, the glacial scenario (*A*) had constricted forest cover compared to the interglacial scenario (*B*). However, many locations experienced extreme minimum temperatures cold enough to restrict plant growth in both scenarios.

limited by low minimum temperatures during the LPIA as they were during the Last Glacial Maximum (10).

Spatial Distribution of Freezing Temperatures and Forest Cover. Freezing minimum temperatures were nearly global in occurrence according to GENESIS V3 simulations (Fig. 1 *A* and *B*). The extent of freezing suggests that it was a limiting factor in forest cover distribution, even in the tropics. Modern tropical forests do not experience freezing temperatures in a typical year (40). Most neotropical tree species are injured or killed at $T_{min} \leq 0$ °C (41). The *Paleo*-BGC model used here does not currently include freeze-related injury and mortality. Therefore, the actual land area covered by forest vegetation during the LPIA may have been substantially less if adaptation to survive leaf and stem freezing had not evolved (Fig. 2 *A* and *B*, Table 2). Particularly during interglacial periods, expansive southern hemisphere land area was available for simulated vegetation based on water balance. Minimum temperature in these locations would have intermittently excluded freeze-intolerant taxa (i.e., hatched area in Fig. 2*B*).

Ecosystem and climate simulations together (*SI Appendix*, Fig. S1) indicate that unglaciated land that could support vegetation but did not freeze was limited during the Pennsylvanian: less than 25% remained above freezing year-round in either scenario (Table 2: excluding areas due to water balance, and where $T_{min} \leq 0$ °C). *Paleo*-BGC predicted that 70% and 95% of unglaciated lands were vegetated (Table 2) in the glacial and interglacial scenarios, respectively. For freeze-intolerant vegetation, however, only 11% of unglaciated land predicted to support vegetation was available in the glacial scenario, and 22% was available in the interglacial scenario. By comparison, the land area that remains above freezing in a typical modern year is considerably more than in either Pennsylvanian extreme [39% total land area excluding Antarctica (40)]. Moreover, in absolute terms, the area of Pangaea covered by forests could have doubled from glacial to interglacial scenarios (Table 2, *SI Appendix*). However, limitations on forest cover due to freezing temperatures may have been compounded by the effect of elevated CO_2 during interglacial periods (42), which was not considered in this study (*Study Caveats*).

Table 2. Land area categories, percentages, and association with fossil occurrences

		Vegetation cover and type fossil occurrences partitioned into zones of minimum temperature (Tmin ranges excluding subsequent colder ranges; °C)				
Scenario		>0	≤0	≤ − 4	≤ − 10	≤ − 40
Glacial: 1. 02 x 10^8km^2 unglaciated land area 70% predicted to support vegetation						
Vegetated area (% of unglaciated land)		**11%**	**16%**	**9%**	**17%**	**17%**
	Fossil taxa					
Pteridophyte lineage	Tracheophyte (other)	0	10	2	5	0
	Fern (other)	0	82	32	74	0
	Lepidodendrales	14	166	242	212	0
	Marattialean tree fern	0	64	48	54	1
	Sphenophyte	14	191	177	276	8
Spermatophyte lineage	Progymnosperms	0	2	1	4	0
	Spermatophyte *incertae sedis*	0	18	16	46	5
	Pteridosperm	2	47	25	41	2
	Medullosan	13	118	103	128	0
	Peltasperm	0	0	3	4	0
	Ginkgophyte	1	0	0	1	1
	Cordaitales	5	30	22	47	13
	Conifer	0	9	18	24	6
Interglacial: 1. 14 x 10^8km^2 unglaciated land area 95% predicted to support vegetation						
Vegetated area (% of unglaciated land)		**22%**	**8%**	**2%**	**22%**	**41%**
Pteridophyte lineage	Tracheophyte (other)	10	7	0	0	0
	Fern (other)	94	94	0	1	0
	Lepidodendrales	277	356	1	0	0
	Marattialean tree fern	87	77	2	1	0
	Sphenophyte	330	318	10	0	8
Spermatophyte lineage	Progymnosperms	3	4	0	0	0
	Spermatophyte *incertae sedis*	21	59	0	2	3
	Pteridosperm	65	49	1	0	2
	Medullosan	196	154	12	0	0
	Peltasperm	0	7	0	0	0
	Ginkgophyte	1	1	0	1	1
	Cordaitales	44	58	2	3	10
	Conifer	10	41	0	0	6

Overall unglaciated land areas and percentages predicted by *Paleo*-BGC to support arboreal vegetation cover are shown alongside scenario descriptions. Minimum temperatures were derived from GENESIS V3 simulations for a glacial scenario with atmospheric CO_2 at 182 ppm and an interglacial with CO_2 at 546 ppm. Vegetated land area was then partitioned into minimum temperature ranges. Percentage of unglaciated land area in each disjoint range of minimum temperature is presented relative to unglaciated land area (percentages and denominator area are bolded, *SI Appendix*, Table S2). The number of plant fossil records is shown for each range of minimum temperature by scenario, based on approximate fossil locations retrieved from the PBDB (http://paleobiodb.org). Genus-level occurrence data are provided in *SI Appendix*, Table S2.

Freeze-tolerance adaptations for at least $T_{min} > -4$ °C appear to have been present in many plant taxa by the Pennsylvanian (Table 2 and Fig. 2). Areas that did not freeze during glacial periods may have been crucial to the survival of some taxa. For example, our simulations indicate that the Cathaysian Islands would have remained above freezing. This may have contributed to the persistence of lycopsids in Cathaysia after they disappeared in tropical Euramerica (43, 44). Nonetheless, a comparison of PBDB fossil locations with ecosystem simulations and climate data suggests that even some tropical communities were likely exposed to some level of freezing at both glacial and interglacial extremes and, therefore, throughout the LPIA. The power of these methods to identify specific plants or communities that experienced freezing is restricted by the limited spatial and temporal resolution of fossil evidence and the boundary conditions used to produce the simulated climate data (*Study Caveats*). In both glacial and interglacial extremes (Table 2 and Fig. 2), however, most PBDB plant macrofossil groups occurred in areas that froze. This information supports the importance of plant freezing as an unstudied component to understanding Late Paleozoic phytogeography.

Continental tropical vegetation would have experienced temperatures cold enough to freeze insulated peripheral tissues, particularly in high elevations in the glacial scenario [Fig. 1*B*, $T_{min} \leq -10$ °C (36)]. During the Late Paleozoic, topography was evolving across the low latitudes of the supercontinent in the CPMR [*Study Caveats* (45)]. At times, CPMR topography may have distinguished LPIA tropical conditions from the modern. For example, in our simulated CPMR, topographic relief produced continuous, continent-wide zones of low temperature near the equator (Fig. 1) that were not tropical in the bioclimatic sense (*SI Appendix*) (40, 46). Modern equivalent bioclimatic zones are limited to a few isolated regions in South America, West Africa, and Malesia (e.g., the Andes) (40). Freezing due to orographic cooling was likely an important limit on tropical forests in the LPIA.

There is an apparent threshold in the fossil data that suggests most Pennsylvanian plants were not freeze-tolerant below $T_{min} \leq -40$ °C (Table 2). This temperature threshold corresponds to the modern boreal climate where tree species have leaf, stem, and physiological adaptations to extreme cold. Even boreal trees are injured by freezing temperatures below −40 °C, particularly when combined with desiccation from wind exposure (41, 47). Only a few modern tree species are considered totally tolerant of freezing and persist in regions that typically experience temperatures at or below this threshold. Notably, in the PBDB, only sphenophytes (but see ref. 32) and spermatophyte fossils (e.g., conifers, cordaitaleans) occurred in locations corresponding to locations with minimum temperatures beyond this threshold (Fig. 2: hatched areas; Table 2: $T_{min} \leq -40$ °C).

Plant fossil taxa in the PBDB were not evenly distributed among areas with simulated freezing temperatures. Overlay of both glacial and interglacial scenarios suggests only a few select genera were found in the coldest areas ($T_{min} \leq -40$ °C; *SI Appendix*, Fig. S2). Examining morphological traits with an eye for freeze adaptation may provide insights into genera found at high-latitude locations. While preservation and collection biases and spatial autocorrelation likely influence these results, the observed threshold may also represent a natural environmental filter due to cold temperatures, as exists today (48). Additional fossil sampling of Carboniferous plants outside of the paleotropics, particularly in the Southern Hemisphere, would further distinguish between these possibilities.

We posit that, along with moisture seasonality, widespread and repeated exposure of plants to freezing temperatures during the Pennsylvanian influenced the evolution of notable aspects of later Paleozoic plant physiology (e.g., in glossopterids and conifers). Plant adaptations to drought can enable plants to resist damage from freezing temperatures and vice versa. Drought and freezing adaptations are mechanistically linked in some instances (49) because, for example, physiological stresses during drought events and freeze-thaw cycles can subject plant vascular systems to similar biophysical pressures. According to our Pennsylvanian simulations, many places that could support significant arboreal vegetation based on water balance (*Paleo*-BGC) would have frozen (GENESIS V3; Table 2 and Fig. 1 and *SI Appendix*, Fig. S1). We further posit that freezing during the LPIA had the potential to select for traits that would enhance survival and reproduction under seasonal drought and freezing during the Late Pennsylvanian (~311 Ma) through the early Permian (~290 Ma). Plant drought- and freeze-resistance likely appeared during earlier climatic extremes, such as the Mississippian [359 to 323 Ma (50)] or possibly the Late Devonian Ice Age [~400 Ma (51)]. However, the LPIA's repeated cycles of moisture seasonality and freezing presented multiple simultaneous stresses. For plants lacking either freeze or drought adaptation, it may have been a particularly restrictive episode and a prolonged period of heightened natural selection in plant evolution.

Freezing Thresholds and Plant Adaptations. The effect of freezing minimum temperatures on forest cover extent is more pronounced when freezing areas are considered as a proportion of vegetated land area (compare Table 1 to *SI Appendix*, Table S1), particularly in the glacial scenario, highlighting the importance of adaptations to freezing during the LPIA. A key plant adaptation that likely conferred both freeze and drought tolerance is small tracheid diameters in stems. This adaptation is found in specific Paleozoic plant groups, such as the cordaitaleans and coniferophytes generally, compared to other Pennsylvanian flora (17). Many extant drought- and freeze-tolerant conifers also have narrow tracheids (52–55). In both glacial and interglacial scenarios, where T_{min} dropped below −10 °C, leaves would have frozen. At less than −40 °C (hatched area in Fig. 2 and Table 2), plants would have had to survive both leaf and stem freezing. After leaf or stem xylem freezing, small xylem lumen diameters [<40 μm (55)] appear to protect plants from freeze-thaw–induced embolism and the concomitant loss of xylem function and productivity (56–58). Also, cordaitaleans and the ancestors of glossopterids (59) may have evolved the capacity to survive peripheral freezing or precipitation seasonality through phenological dormancy (e.g., deciduousness) by the Carboniferous. Phenological dormancy is thought to have appeared in cordaitaleans and Glossopteridales by the Permian, as evidenced by growth rings in particular (60–63). "False growth rings" described in Carboniferous cordaitaleans (reviewed by ref. 64) may be explained, in an otherwise favorable environment, by daily timescale freezing events. Overnight freezes may have slowed or stopped cambial activity and affected plants even at equatorial latitudes (Fig. 1). Furthermore, a coniferophyte from the Late Pennsylvanian (65) had leaf traces cut off at the first growth-ring boundary, indicating leaf abscission after the first year and suggesting deciduousness. Some sphenophytes, mainly herbaceous taxa with narrow tracheids (66), may have been freeze adapted similar to some extant *Equisetum* species (67). For example, *Arthropitys* bear vallecular canals (68), which appear to be an adaptation to manage extracellular ice formation in *Equisetum hyemale* (69). Using another strategy, sphenophytes with broad tracheids like *Sphenophyllum* (48) may have survived freeze or droughts despite nonadapted above-ground organs by resprouting from rhizomes where/when soil temperatures were favorable (67, 70). All of these characteristics would be adaptive for both water- and low-temperature stress. This adaptive synergy has perhaps contributed to the relative morphological conservation of sphenophyte and, especially, coniferophyte lineages today, compared to many other lineages of late Paleozoic origin (67, 71).

Cordaitaleans and some sphenophytes may have survived some of the harshest cold temperatures. Nonetheless, all plant groups examined in this study were likely exposed to temperatures down to −4 °C (Table 2, interglacial). This exposure suggests that peripheral freezing damage sustained by these Carboniferous plants did not prevent their growth and propagation or that they were adapted to avoid injury at some subfreezing temperatures. Adaptation to maintain transient internal supercooling of water would be required for survival in locations where $T_{min} \leq 0$ °C. The cumulative area affected by freezing was 59% of unglaciated land predicted to support vegetation in the glacial scenario and 73% in the interglacial scenario (cumulative up to $T_{min} \leq 0$ °C in Table 2). Evidence of the biochemistry of this adaptation may not be directly detectable in the fossil record. Still, anatomical features that were previously interpreted as conferring resistance to drought stress may have played an additional role in supporting freeze tolerance. For example, sunken stomata found within some Carboniferous plants (e.g., *Macroneuropteris scheuchzeri*) may have served to limit water loss under low temperatures (36, 72). At colder temperatures ($T_{min} \leq -4$ °C), some plant tissues would have frozen, generally requiring morphological adaptations to survive (41).

The cumulative area of unglaciated land with predicted vegetation and minimum temperatures ≤ −4 °C, where uninsulated peripheral tissue would freeze, was 43% in the glacial and 65% in the interglacial scenarios (Table 2: cumulative up to $T_{min} \leq -4$ °C). This included regions in the tropics. Leathery leaves of gymnosperms (51) and reinforced internal leaf tissue (hypodermal sclerenchyma) in several Carboniferous cordaitalean leaf taxa may have functioned as peripheral insulation (73). However, insulating structures in modern plants cannot prevent live tissue in leaves from freezing at temperatures < −10 °C beyond daily timescales (36). Excepting desiccation-tolerant vegetation that may be protected from freezing when water content is low (74, 75), temperatures below −4 °C overcome freezing-point depression afforded by intercellular solutes. Prolonged temperatures below this threshold require adaptations that allow recovery from freezing, such as deciduousness and narrow tracheids. Freezing adaptations, furthermore, are varied and involve synergies of whole plant physiology. For example, dead retained foliage insulates the stem against freezing in tropical alpine taxa (76), and high pubescence on leaves can raise leaf temperatures up to 10 °C above ambient air (77). Furthermore, more detailed anatomical evaluations of freeze adaptation in Carboniferous taxa will improve phytogeographic reconstructions for the period.

Hypothesized Impact of Plant Freezing on Landscape Hydrology. As the evolution of freeze-tolerance in Paleozoic vascular plants is not well established, we impose a global −4 °C plant freezing threshold and present a case study of the potential effects on hydrology. Our unmodified *Paleo*-BGC simulations provide a maximum extent of global forest cover that may be refined by considering additional limiting factors. Freezing temperatures in the Pennsylvanian would have reduced regional support of arboreal vegetation. The actual contraction of forest cover would have depended on the coincidence of existing plant freeze adaptations and minimum temperatures. We present a simplified case to explore some potential effects of freeze stress on the Earth system. Overlaying the location of PBDB plant fossils on GENESIS V3 predicted interglacial minimum temperatures supports the possibility that many Paleozoic taxa were intolerant of temperatures ≤ −4 °C (Table 2 and *SI Appendix*, Fig. S1). As a bounding case, therefore, we assume that most plants were not adapted to temperatures below −4 °C. Under this assumption, a single night of temperatures below −4 °C would have killed most vascular plants. We believe the resulting contraction of our projected forest cover estimate represents a useful and convenient estimate of the minimum extent of forest cover. Below the ≤ −4 °C threshold, many plants cannot avoid cell freezing and plasma membrane rupture and, therefore, require morphological adaptations against freezing (36). This provides an avenue for future paleontological evaluation. Furthermore, during the Last Glacial Maximum, contraction of forest cover is thought to have been tracked by the expansion of grass- or sclerophyll shrub-dominated biomes (10). These taxa, which are important controls on surface erosion today, may not have functional equivalents in the Carboniferous. Affected regions may have remained minimally vegetated, altering hydrologic processes.

During the LPIA, large areas were affected by freezing temperature minima of −4 °C and colder according to GENESIS V3 simulations of both peak glacial and interglacial periods (Fig. 1 and Table 2). This would have resulted in the total mortality of freeze-intolerant arboreal vegetation and loss of forest cover, resulting in rapid and dramatic environmental changes (*Materials and Methods*). In reality, regions with diverse vegetation likely experienced widespread but patchy deforestation. Nonetheless, in the coldest years, in regions dominated by freeze-intolerant vegetation, near-synchronous die-off in forests would have resulted in loss of forest cover and evapotranspiration. Subsequent soil destabilization would have compounded increases in soil incident precipitation and soil moisture to promote erosion, transport of terrigenous material, fresh mineral exposure, and chemical weathering. In warmer months and years (i.e., under average conditions), productivity and plant recolonization would have reversed these soil effects but then been interrupted again by freezes, depending on successional patterns. The conditions producing these extreme minimum temperature events and the resulting alternating vegetative states would have persisted, on a subeccentricity timescale, for tens of thousands of years (15). Full forest recovery in freeze-affected regions would not occur until minimum temperatures persistently rose above threshold values that allowed freeze-intolerant forms to recolonize. Alternatively, freeze-tolerant or frost-avoidant forms evolved, colonized, and dominated freeze-affected regions. Persistent forest vegetation cover reduction by freezing temperatures would have affected surface hydrology. Changes in transpiration, canopy interception, and canopy evaporation affect soil water balance and runoff. These processes are represented in *Paleo*-BGC, allowing us to estimate the effect of vegetation loss on runoff.

An upper bound for freeze-induced change in runoff (Δ_R) was estimated using *Paleo*-BGC (*Materials and Methods*). We imposed total freeze-induced vegetation loss where $T_{min} \leq -4$ °C, which caused a net global increase in surface runoff of 5.7% for the glacial scenario and 6.1% for the interglacial scenario. In absolute terms, global net increases in runoff for the glacial and interglacial scenarios were equivalent to 30% and 47% of the Amazon River's current average annual discharge (78) compared to *Paleo*-BGC: $2.0 \times 10^6 m^3 y^{-1}$ and $3.1 \times 10^6 m^3 y^{-1}$ (Fig. 3).

Changes in runoff, however, were regionally heterogeneous. Where runoff increased due to plant freezing (Fig. 3), freshwater inputs to coastal marine environments would have decreased salinity of surface waters and decreased near-shore carbonate $\delta^{18}O$ beyond abiotic factors alone (79–81). Predicted increases in mineral, sediment, organic matter, and nutrient exports with large pulses of freshwater to riverine, riparian, and coastal marine environments may be detectable in the geologic record. For example, they may appear as local or regional stratigraphic or isotopic anomalies, such as excursions in $\delta^{34}S$ and marine carbonate $\delta^{13}C$ (79, 80). However, the composition of this runoff would have depended on the properties of the catchments through which it flowed and how those catchments were affected by vegetation freezing (30, 82).

Freeze-induced change in runoff (Δ_R) varied considerably across supercontinent Pangaea and between glacial and interglacial scenarios (Fig. 3). This case study demonstrates the potential for

interactions of climate and vegetation productivity to cause considerable location-specific differences in surface water discharge rates (Fig. 3). The highest Δ_R of the glacial scenario in our case study occurred in the CPMR (*Study Caveats*). Simulated orographic precipitation and cooler temperatures in the CPMR produced vegetation and high transpiration under average conditions. That vegetation was eliminated by freezing under extreme conditions. This phenomenon was absent in the interglacial scenario, wherein the CPMR remained above −4 °C. Similarly, high Δ_R spanned the southern midlatitudes of Gondwanaland in the interglacial scenario (Fig. 3 *C* and *D*), whereas in the glacial scenario, Δ_R was considerably muted by the lack of precipitation in the eastern part of that region.

High- and middle-latitude locations under glacial climate showed no predicted difference in runoff, which was likely due to

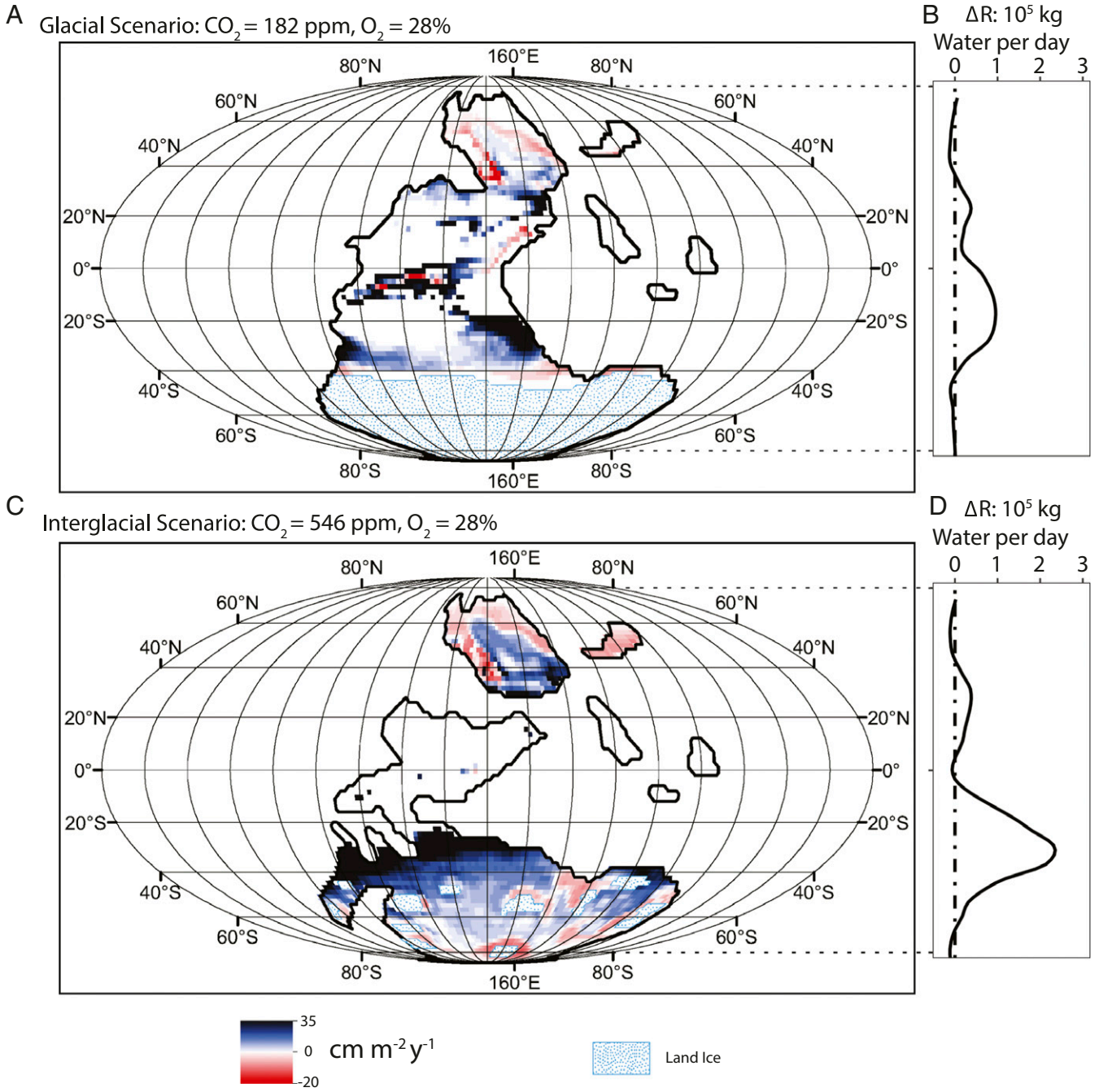

Fig. 3. Change in runoff due to one possible freeze intolerance threshold (T_{min}) of plants in two climate scenarios of the Pennsylvanian. A general circulation model (GENESIS V3) was used to estimate daily minimum temperature globally, at 2-degree (longitude, latitude). Maps are in the Molleweide projection. Data from GENESIS V3 was used as input to an ecosystem process model (*Paleo*-BGC) that was run with and without plants. For each scenario, the difference in runoff between simulations without plants and with plants ($\Delta_R = R_{no\ plants} - R_{plants}$) where the minimum temperature dropped below −4 °C. Where minimum temperature remained above −4 °C, Δ_R was set to zero. Presented is Δ_R at 2-degree longitude/latitude resolution (*A* and *C*) and summarized by latitude (*B* and *D*). Regionally varying changes in runoff due to freeze-mortality of plants may have impacted the Carboniferous geologic and paleobotanical records differently between peak glacial periods and interglacial periods.

the locations being too dry to support simulated arboreal plants or produce runoff in *Paleo*-BGC. A few locations in the low latitudes and the northern Pangaean peninsula (Angaraland) between the midcontinent and coast showed considerably decreased runoff. In these locations, modeled transpiration was less than soil evaporation if vegetation was excluded.

In our modeled CPMR, orographic effects in regions of high relief interacted with our assumed vegetation freeze-threshold to produce high Δ_R (Fig. 3). These model results may be biased by our simplified representation of topography in the CPMR (83), which evolved throughout the LPIA (45) (*Materials and Methods*, *Study Caveats*). However, the scale of Δ_R in our case study supports recent modeling in suggesting that CPMR topography could have been a key factor in LPIA hydrology and geochemistry (81). Furthermore, these results suggest these factors interacted with, and were modulated by, phytogeography. The strongest geologic evidence for, or against, an actual vegetation freeze-threshold may have been produced in these regions. Topographic uplift could have increased mineral weathering efficiency (30, 45) and also increased runoff due to freeze-induced forest die-off. This interaction may have increased dissolved matter discharge (82). The effect of weathering on climate would have depended on underlying lithologies and transport to marine locales (32, 84).

In contrast to the CPMR, many midlatitude areas lacked plant-available water, and thus vegetation, during the glacial scenario. These regions had little to no Δ_R. This produced an east-west asymmetry in the glacial scenario that was absent in the interglacial scenario. Thus, freeze-induced freshwater yield (Δ_R) may have fluctuated with glacial glacial–interglacial cycles during interglacial cycles. Unknown forest vegetation responses to climate complicate interpretation of paleo-record signals, including geologic indicators and isotopic differences. Our case study supports vegetation freeze-mortality as one such complicating factor.

Finally, plant freeze intolerance could have enhanced peat formation, impacting carbon sequestration and atmospheric pCO_2, particularly during glacial times (11). Under average glacial conditions, high insolation and moisture resulted in high forest productivity in the tropics (Fig. 2, *SI Appendix*). Sporadic extreme cold events would result in cyclic, regional-scale die-off and regrowth of freeze-intolerant arboreal lowland plants. The result would be increased in situ organic matter deposition, reduced transpiration, and increased soil moisture across broad depositional areas (Figs. 1 and 3). Cold temperatures would also have reduced heterotrophic respiration and decomposition. Together, these factors support (85) the formation of peat swamps during the LPIA glacial periods. This pattern would have been reduced or absent in the interglacial tropics given warmer lowlands (Fig. 1*B*). This study suggests multiple roles of cold temperatures in organic matter accumulation during glacial periods of the LPIA: as a depositional trigger and a mechanism of dead organic matter production.

Conclusions

Freezing is a critical threshold that is lethal to some plants with less than 24-h exposure. Consideration of freezing stress on plants is only possible because of the ability of GCMs to estimate daily temperature extremes in deep time. This consideration augments previous paleoecosystem reconstructions based on paleobotanical, sedimentological, and geochemical data (72). With freeze impacts included, the climatic perturbations of the terminal phase of the LPIA may have been a crucible for plant evolution. Therein, important anatomical and physiological adaptions began their rise to prominence in terrestrial ecosystems, shaping the subsequent evolutionary history of plant life. During our proposed cycles of freezing and vegetation recovery, sporadic forest cover loss would have increased soil erosion, exposure of fresh minerals, and enhance chemical weathering. Such freezing events occurred in the context of years or decades of vegetation regrowth under average conditions when all these effects on soil would be reversed. These processes may be detectable, for example, in the marine record of freshwater and sediment influx.

We have taken preliminary steps to highlight the importance of plant freeze-tolerance traits and characterize the effects of freezing on related Earth system processes, specifically phytogeography and hydrology. Field-based paleontological data will help clarify the phytogeography and morphological characters related to drought and potential freeze-tolerance presented here. In addition, improved paleotopographic information for the Carboniferous, as well as other time periods, is needed to better constrain the climatic and hydrographic environment in which ancient plants lived and evolved. Ancient plant function is better understood through the lens of biophysical principles, and Earth system models of deep time (86) should represent simulated vegetation with as much historical authenticity as possible through the use of process-appropriate timescales.

Materials and Methods

See *SI Appendix*, Fig. S1, for a graphical presentation of the methods. Forest cover in the Pennsylvanian was simulated for a global grid consisting of 2° × 2° cells using the ecosystem process model *Paleo*-BGC (24), a modified version of the ecosystem model BIOME-BGC (87, 88), driven by daily data derived from GENESIS V3 (26, 27). The *Paleo*-BGC model (24) includes variable atmospheric pO_2, mesophyll conductance important for plants with thickened leaves, and leaf hydraulic conductivity to account for simple and complex vascular pathways. Measurements of leaf carbon to nitrogen ratio (C:N; $kg\ \ kg^{-1}$) were derived from preserved cuticular material. Maximum stomatal conductance (g_{smax}; $mol\,m^{-2}s^{-1}$) was determined from stomatal density and size of leaf fossil impressions. Fossil measurements were collected for Pennsylvanian representative plant-fossil taxa (described in refs. 2 and 23) including lycopsids, sphenophytes, pteridosperms, stem-group marattialean tree ferns (tree ferns), and early-diverging coniferophytes [cordaitaleans (23, 32)]. SLA ($m^2\,kg\,C^{-1}$) and related leaf attributes, important for converting carbon allocated to leaves to leaf area, were estimated using measured leaf C:N to SLA relationships from extant relatives (89, 90). Boundary layer conductance (g_b; $\mu mol\,s^{-1}Pa^{-1}m^{-2}$) was estimated from the mean leaf or leaflet width (91). For leaf mesophyll conductance (g_m; $\mu mol\,s^{-1}Pa^{-1}m^{-2}$), a single mean value of 0.273 mol $H_2Om^{-2}s^{-1}$ was used as a basis for measurements of leaf air space, leaf thickness, mean mesophyll cell width, and cell-wall thickness of leaf fossil cross-sections of Pennsylvanian taxa (24). Finally, leaf hydraulic conductivity values (K_{leaf}; $mmol\,m^{-2}s^{-1}MPa^{-1}$) were calculated from an empirical relationship (92) using minimum and maximum leaf mesophyll pathlength derived from leaf fossil cross sections (92).

Data were generated by GENESIS V3 as described in refs. 15, 93, and 94. Minimum temperatures were averaged over terrestrial locations that were not covered by glacial ice. Inputs taken for *Paleo*-BGC included daily maximum, minimum, and average temperature (T_{min}, T_{max}, and T_{ave}), precipitation, and shortwave radiation for 10 y. Vapor pressure deficit, a required input for *Paleo*-BGC, was calculated using T_{min} and T_{ave} in the modified Tetens equation (95) for each grid cell. Finally, daily daylength was derived for each grid cell based on latitude and year day (91). Two climate scenarios were evaluated, intended to provide a characterization of the glacial and interglacial intervals. One climate scenario with glacial ice and CO_2 of 182 ppm is referred to as the glacial, and one with reduced glacial ice and CO_2 of 546 ppm is referred to as the interglacial. For both scenarios, atmospheric oxygen was set to 28%, which is considered a maximum pO_2 for this period based on recent modeling (96).

Landmasses and glacial extents were specified after the description of Ziegler, Hulver, and Rowley [(97), for ~290 Ma, earliest Artinskian]. Vegetated land area was mapped following a two-part categorization process for each unglaciated terrestrial grid cell. First, LAI predicted by *Paleo*-BGC at each grid point was averaged across all plant groups and categorized as "vegetated" or "bare" based on a threshold LAI value of 0.1 [minimum LAI measured by (98)] excepting the grassland biome (*SI Appendix*). Second, daily minimum temperature thresholds were set at levels relevant to modern plant freeze adaptations where freezing injury is likely in peripheral tissues of plants incapable of maintaining transient internal supercooled water [$T_{min} \leq 0$ °C; (36, 41)], where peripheral freeze injury would occur in

plants without insulating tissue or adaptations to maintain persistent supercooling ($T_{min} \leq -4$ °C), where freeze injury is likely in peripheral tissues and stems of plants without insulating tissue ($T_{min} \leq -10$ °C), and at which homogeneous nucleation is unavoidable and xylem adaptations to avoid freeze/thaw embolism are required for survival ($T_{min} \leq -40$ °C).

Where vegetation predicted by *Paleo*-BGC coincided with these temperature thresholds, we considered plants to have experienced some form of freeze damage. The area covered by freezing-affected locations was then calculated by summing the area of 2° × 2° grid cells in that T_{min} category. Grid cell areas (A) were approximated as equilateral trapezoids centered on the geographic coordinates (longitude, latitude) of the grid cell: $A \cong 222^2 \cdot \frac{\cos(lat+1)+\cos(lat-1)}{2}$. This accounts for varying longitude lengths across Earth's spherical surface. The length of one degree of longitude at a given latitude is approximated as the cosine of degrees latitude times the length of a degree of longitude at the equator (~111 km). The side-lengths were then calculated at latitudes one degree north and south from the center latitude of the grid cell, respectively, and multiplied by the approximate length of a two-degree latitude ($\sim 2 \cdot 111\,km$).

We compared our simulated vegetation cover with plant fossil occurrence for the Pennsylvanian from the PBDB (downloaded from http://paleobiodb.org 28 May 2019; Fig. 1 and *SI Appendix*) by using several search terms associated with well-known Carboniferous tracheophyte taxa and selecting the time interval "Pennsylvanian." A total of 3,568 plant fossil occurrences were found and sorted into broad groups (taxa and associations in *SI Appendix*, Table S2).

Finally, we assessed a case study of the maximum potential impact of freeze-limited plant biogeography on steady-state surface runoff. Site water balance in *Paleo*-BGC is estimated using a simple bucket model that does not consider infiltration, percolation, or lateral flow. Rather, surface runoff (R) is estimated from the remainder of water left in the soil after evapotranspiration that is in excess of maximum volumetric water content. The lack of inclusion of lateral flow is somewhat mitigated by the large spatial scale. Each grid cell is roughly the size of a large watershed; much of the lateral flow and surface flow would be consolidated into the same river outflow from that grid cell.

We calculated the percent change in runoff as follows. The change in runoff was calculated as the difference between annual runoff in *Paleo*-BGC simulations without plants and with plants ($\Delta_R = R_{no\ \ plants} - R_{plants}$). This was calculated for grid cells where $T_{min} \leq -4°C$ and set to zero for warmer grid cells. Removal of forest vegetation assumed freeze intolerance and exclusion from locations where $T_{min} \leq -4°C$. Percent change in runoff ($\%\Delta_R$) was calculated as the cumulative change in runoff, weighted by the approximate area for each grid cell, divided by the cumulative, area-weighted runoff from the unmodified *Paleo*-BGC simulations (R_{plants}). The resulting $\%\Delta_R$ expresses the potential impact of freeze-mortality on hydrology due to the difference between forested and barren states. This calculation is only a measure of the difference between end-states and does not consider the intermediate processes associated with the transition from vegetated to barren. Once plant mortality has occurred, the timescale of this transition may vary from years to decades or longer as plant communities come and go in response to freezing temperature. The resultant impact would also be locally dependent on a complex set of feedbacks involving biotic and abiotic factors (99) including precipitation intensity, gradient, soil formation rate, nutrient availability, community composition, and rhizosphere properties.

Generally, locations with little vegetation and/or precipitation show a lower change in runoff due to the removal of plants. Conditions resulting in positive Δ_R (i.e., increased runoff) were favorable for simulated vegetation growth, such as areas with high precipitation. Under these conditions, high transpiration rates reduced soil moisture and runoff, despite high precipitation. Removing plants, therefore, increased runoff. Conditions producing negative Δ_R (i.e., decreased runoff) were marginal due to low temperature but allowed sufficient transpiration to produce vegetation growth. Removing plants allowed higher soil incident radiation and more soil evaporation than would have been lost due to transpiration, leading to lower runoff.

Latitudinal trends in Δ_R were assessed by summing values across all grid cells at each latitude. These quantitative differences represent the runoff in two stable landscapes under the same conditions except for the presence or absence of vegetation. The instantaneous change due to the novel denudation of a landscape is not captured by Δ_R. Furthermore, this calculation does not consider the sequence of regional transitions between vegetated and nonvegetated states that would likely occur during the onset or recession of the glacial climate. In general, if minimum temperatures advanced in latitude toward the equator along with the cooling climate, landscape transitions would cycle on a subeccentricity timescale (~10^4 to 10^5 years). For example, freezing minimum temperatures occurred at around 25° in the interglacial scenario (Fig. 1) and advanced to about 15° by the glacial scenario. A region spanning 1° of latitude would then transition over the course of 10^3 to 10^4 years. The timescale of climate change is, however, the result of a complex dynamic system; land area in the LPIA would have been subject to differential heating and cooling patterns due to other interacting phenomena like ocean circulation and continental effects.

Study Caveats. The minimum temperatures and precipitation described herein are subject to uncertainties associated with the GENESIS V3 GCM itself and the boundary conditions (paleogeography, paleotopography, and CO_2) used for these simulations. For example, uncertainties in atmospheric CO_2 may affect simulated minimum temperatures, glacial ice cover, ocean level, and vegetation cover (100). Furthermore, the GENESIS V3 GCM may be less sensitive to atmospheric CO_2 than other models [e.g., Community Earth System Model (101, 102)].

Continental arrangement and paleotopography used in our GCM simulations represent a single point in time, 290 Ma, described in refs. 15, 93, and 94. Furthermore, the paleotopography we utilized does not capture the evolution of the CPMR, which is thought to have been largely eroded in some regions by the Late Pennsylvanian (45). Rather, it serves as a bounding case with maximum uplift. Considering the importance of the tropics to the biosphere, additional studies should be performed to determine the sensitivity of vegetation to tropical topographic heterogeneity at the time. Shorelines, land ice, and CO_2 are intended to represent extreme conditions associated with maximum and minimum glaciation.

The models used to infer LAI here, GENESIS V3 and *Paleo*-BGC, are not coupled. As a result, locations are hydrologically disconnected, and water available to vegetation may be systematically altered as a result. The spatial scale of this study is roughly similar to that of a watershed. This may limit the error resulting from our use of uncoupled models, as water may have been unavailable to vegetation due to percolation and stream outflow. An additional caveat to our use of uncoupled models is that vegetation differences do not affect surface dynamics of moisture, radiation, or mass transfer. Efforts are currently underway to integrate era-appropriate vegetation into Earth system models.

The *Paleo*-BGC model estimated higher LAI in tropical montane regions than some modern measurements for the same biome (Table 1). Notably, our LAI estimates are not intended to represent any particular plant or community. As the mean of LAI from several plant groups, our estimates are intended to represent "generic Carboniferous forest vegetation." Actual plant and community LAI are influenced by many factors, including canopy structure, which is not considered here. We posit that high *Paleo*-BGC values are the result of the fossil-based physiological parameterization of *Paleo*-BGC as well as the paleotopographic parameterization of GENESIS V3 (83). Here, we use taxa-specific scaling relationships with C:N to estimate SLA (24). *Paleo*-BGC scales LAI from leaf C and SLA. This produced high LAI in taxa with low $C:N_{leaf,}$ including Marattialean tree ferns, which had the highest LAI. Fossil C:N ratios may also be altered during preservation (see physiological characterization in ref. 24). Estimation of leaf economic traits in fossil taxa remains a considerable challenge. Future experiments with *Paleo*-BGC that compare estimates of LAI based on additional methods for estimating SLA [e.g., using relationships with petiole width, adaxial epidermal density, and cuticle thickness (37, 38)] may improve estimates of LAI and vegetation cover. Additionally, paleotopography is not well constrained in the Pennsylvanian and may result in overestimation of equatorial orographic precipitation and, therefore, LAI. Finally, interglacial estimates of LAI may be further inflated, as the exacerbation of leaf freezing associated with elevated CO_2 has not been accounted for here (42, 103).

Our analysis of freeze tolerance does not consider interactions of plant organs such as marcescent leaves' insulation of stems in some extant taxa (104). As a more detailed understanding of ancient whole plant physiology emerges, evaluation of the totality of plant freeze tolerance will further improve the estimation of ancient vegetation cover and plant distributions. Comparisons to modern distributions will also become clearer.

The synthesis of modeling data and fossil occurrence data should be interpreted with care due to limitations on the temporal resolution of direct geological and paleobotanical evidence in deep time. As stated, our modeling is not intended to capture a specific point in time but rather is based on generalized geological evidence from glacial-interglacial cycles of atmospheric composition and paleogeography. In addition, fossil occurrences from the PBDB (http://pbdb.org) may represent long time intervals and large areas of spatial origin (i.e., allochthonous), which can distort the apparent picture of plant distribution. Because the PBDB relies on contributions from many sources, misidentifications of fossils temporally, spatially, or taxonomically are

also possible. Therefore, the coincidence of minimum temperatures with any particular plant fossil occurrence should be taken only as a hypothesis rather than proof that a fossil taxon may have experienced that environmental stress.

Data Availability. Data generated by GENESIS V3 used to produce *Paleo*-BGC inputs and the *Paleo*-BGC output files are available on Dryad. The scripts required to adapt GENESIS V3 data and perform parameterized *Paleo*-BGC runs in parallel using a cluster computer are provided at GitHub, https://github.com/wjmatthaeus/bgc_utils (105). The *Paleo*-BGC model description is provided by ref. 24. *Paleo*-BGC model code can be found along with current parameter files at GitHub, https://github.com/josephdwhite/paleo-bgc (106). Model code and simulation output data have been deposited in Zenodo, https://doi.org/10.5281/zenodo.4686065 (107), and Dryad, https://doi.org/10.5061/dryad.qnk98sfgj (108).

ACKNOWLEDGMENTS. W.J.M. acknowledges Baylor University High Performance and Research Computing Services group for their assistance in the simulations presented here. We thank the Numerical Terradynamic Simulation Group at the University of Montana for the development of the original BIOME-BGC model. These data and findings were supported by NSF Earth Sciences Grants EAR-1338247 (to J.D.W.), EAR-1338281 (to I.P.M.), EAR-1338200 (to C.J.P.), and EAR-1338256 (to M.T.H.) and European Research Council ERC-2011-StG and 279962-OXYEVOL (to J.C.M.). We thank the Editor and Reviewers for their valued contributions.

1. W. Qie, T. J. Algeo, G. Luo, A. Herrmann, Global events of the Late Paleozoic (Early Devonian to Middle Permian): A review. *Palaeogeogr. Palaeoclimatol. Palaeoecol.* **531**, 109259 (2019).
2. J. P. Wilson *et al*., Dynamic Carboniferous tropical forests: New views of plant function and potential for physiological forcing of climate. *New Phytol.* **215**, 1333–1353 (2017).
3. H. J. Falcon-Lang, A. R. Bashforth, Pennsylvanian uplands were forested by giant cordaitalean trees. *Geology* **32**, 417–420 (2004).
4. B. A. Thomas, C. J. Cleal, Distinguishing Pennsylvanian-age lowland, extra-basinal and upland vegetation. *Palaeobiodivers. Palaeoenviron.* **97**, 273–293 (2017).
5. W. A. DiMichele, I. P. Montañez, C. J. Poulsen, N. J. Tabor, Climate and vegetational regime shifts in the late Paleozoic ice age earth. *Geobiology* **7**, 200–226 (2009).
6. R. Pearce, Plant freezing and damage. *Ann. Bot. (Lond.)* **87**, 417–424 (2001).
7. S. P. Harrison *et al*., Ecophysiological and bioclimatic foundations for a global plant functional classification. *J. Veg. Sci.* **21**, 300–317 (2010).
8. W. Larcher, H. Bauer, "Ecological significance of resistance to low temperature" in *Physiological Plant Ecology I, Encyclopedia of Plant Physiology (New Series)*, O. L. Lange, P. S. Nobel, C. B. Osmond, H. Ziegler, Eds. (Springer Berlin Heidelberg, 1981).
9. T. J. Crowley, S. K. Baum, Modeling late Paleozoic glaciation. *Geology* **20**, 507–510 (1992).
10. I. C. Prentice, S. P. Harrison, P. J. Bartlein, Global vegetation and terrestrial carbon cycle changes after the last ice age. *New Phytol.* **189**, 988–998 (2011).
11. W. A. DiMichele, Wetland-dryland vegetational dynamics in the Pennsylvanian ice age tropics. *Int. J. Plant Sci.* **175**, 123–164 (2014).
12. A. R. Bashforth, C. J. Cleal, M. R. Gibling, H. J. Falcon-Lang, R. F. Miller, Paleoecology of Early Pennsylvanian vegetation on a seasonally dry tropical landscape (Tynemouth Creek Formation, New Brunswick, Canada). *Rev. Palaeobot. Palynol.* **200**, 229–263 (2014).
13. K. Willis, J. McElwain, *The Evolution of Plants* (OUP Oxford, 2014).
14. G. Le Hir *et al*., The climate change caused by the land plant invasion in the Devonian. *Earth Planet. Sci. Lett.* **310**, 203–212 (2011).
15. D. E. Horton, C. J. Poulsen, I. P. Montañez, W. A. DiMichele, Eccentricity-paced late Paleozoic climate change. *Palaeogeogr. Palaeoclimatol. Palaeoecol.* **331–332**, 150–161 (2012).
16. D. J. Beerling, J. C. McElwain, C. P. Osborne, Stomatal responses of the 'living fossil' Ginkgo biloba L. to changes in atmospheric CO2 concentrations. *J. Exp. Bot.* **49**, 1603–1607 (1998).
17. J. P. Wilson, A. H. Knoll, N. M. Holbrook, C. R. Marshall, Modeling fluid flow in Medullosa, an anatomically unusual Carboniferous seed plant. *Paleobiology* **34**, 472–493 (2008).
18. P. J. Franks, D. J. Beerling, Maximum leaf conductance driven by CO2 effects on stomatal size and density over geologic time. *Proc. Natl. Acad. Sci. U.S.A.* **106**, 10343–10347 (2009).
19. C. K. Boyce, J.-E. Lee, T. S. Feild, T. J. Brodribb, M. A. Zwieniecki, Angiosperms helped put the rain in the rainforests: The impact of plant physiological evolution on tropical biodiversity. *Ann. Mo. Bot. Gard.* **97**, 527–540 (2010).
20. P. J. Franks *et al*., Sensitivity of plants to changing atmospheric CO_2 concentration: From the geological past to the next century. *New Phytol.* **197**, 1077–1094 (2013).
21. J. P. Wilson, Modeling 400 million years of plant hydraulics. *The Paleontological Society Papers* **19**, 175–194 (2013).
22. J. C. McElwain, C. Yiotis, T. Lawson, Using modern plant trait relationships between observed and theoretical maximum stomatal conductance and vein density to examine patterns of plant macroevolution. *New Phytol.* **209**, 94–103 (2016).
23. I. P. Montañez *et al*., Climate, pCO2 and terrestrial carbon cycle linkages during late Palaeozoic glacial–interglacial cycles. *Nat. Geosci.* **9**, 824–828 (2016).
24. J. D. White *et al*., A process-based ecosystem model (Paleo-BGC) to simulate the dynamic response of late carboniferous plants to elevated O2 and aridification. *Am. J. Sci.* **320**, 547–598 (2020).
25. J. D. Richey *et al*., Modeled physiological mechanisms for observed changes in the late Paleozoic plant fossil record. *Palaeogeogr. Palaeoclimatol. Palaeoecol.* **562**, 110056 (2021).
26. S. L. Thompson, D. Pollard, Greenland and antarctic mass balances for present and doubled atmospheric CO_2 from the GENESIS version-2 global climate model. *J. Clim.* **10**, 871–900 (1997).
27. J. R. Alder, S. W. Hostetler, D. Pollard, A. Schmittner, Evaluation of a present-day climate simulation with a new coupled atmosphere-ocean model GENMOM. *Geosci. Model Dev.* **4**, 69–83 (2011).
28. G. P. Asner, J. M. O. Scurlock, J. A. Hicke, Global synthesis of leaf area index observations: Implications for ecological and remote sensing studies: *Global leaf area index. Glob. Ecol. Biogeogr.* **12**, 191–205 (2003).
29. D. W. Inouye, The ecological and evolutionary significance of frost in the context of climate change. *Ecol. Lett.* **3**, 457–463 (2000).
30. K. Maher, C. P. Chamberlain, Hydrologic regulation of chemical weathering and the geologic carbon cycle. *Science* **343**, 1502–1504 (2014).
31. D. E. Ibarra, S. Moon, J. K. Caves, C. P. Chamberlain, K. Maher, Concentration–discharge patterns of weathering products from global rivers. *Acta Geochimica* **36**, 405–409 (2017).
32. J. D. Richey *et al*., Influence of temporally varying weatherability on CO2-climate coupling and ecosystem change in the late Paleozoic. *Clim. Past* **16**, 1759–1775 (2020).
33. M. Kottek, J. Grieser, C. Beck, B. Rudolf, F. Rubel, World Map of the Köppen-Geiger climate classification updated. *metz* **15**, 259–263 (2006).
34. T. Luo *et al*., Leaf area index and net primary productivity along subtropical to alpine gradients in the Tibetan Plateau: Leaf area index and productivity along Tibetan transects. *Glob. Ecol. Biogeogr.* **13**, 345–358 (2004).
35. S. Opluštil, C. J. Cleal, J. Wang, M. Wan, Carboniferous macrofloral biostratigraphy—An overview. *Geol. Soc. Spec. Publ.*, **143**, 261–302 (2020).
36. W. Larcher, *Physiological Plant Ecology* (Springer, ed. 3, 2003).
37. D. L. Royer *et al*., Fossil leaf economics quantified: Calibration, Eocene case study, and implications. *Paleobiology* **33**, 574–589 (2007).
38. M. Haworth, A. Raschi, An assessment of the use of epidermal micro-morphological features to estimate leaf economics of Late Triassic–Early Jurassic fossil Ginkgoales. *Rev. Palaeobot. Palynol.* **205**, 1–8 (2014).
39. W. K. Soh *et al*., Palaeo leaf economics reveal a shift in ecosystem function associated with the end-Triassic mass extinction event. *Nat. Plants* **3**, 17104 (2017).
40. K. J. Feeley, J. T. Stroud, Where on Earth are the "tropics"? *Front. Biogeogr.* **10**, e38649 (2018).
41. A. Sakai, W. Larcher, *Frost Survival of Plants* (Springer Berlin Heidelberg, 1987).
42. D. L. Royer, C. P. Osborne, D. J. Beerling, High CO2 increases the freezing sensitivity of plants: Implications for paleoclimatic reconstructions from fossil floras. *Geology* **30**, 963 (2002).
43. J. Hilton, C. J. Cleal, The relationship between Euramerican and Cathaysian tropical floras in the Late Palaeozoic: Palaeobiogeographical and palaeogeographical implications. *Earth Sci. Rev.* **85**, 85–116 (2007).
44. H. W. Pfefferkorn, J. Wang, Early Permian coal-forming floras preserved as compressions from the Wuda District (Inner Mongolia, China). *Int. J. Coal Geol.* **69**, 90–102 (2007).
45. M. Roscher, J. W. Schneider, Permo-Carboniferous climate: Early Pennsylvanian to Late Permian climate development of central Europe in a regional and global context. *Geol. Soc. Lond. Spec. Publ.* **265**, 95–136 (2006).
46. H. E. Beck *et al*., Present and future Köppen-Geiger climate classification maps at 1-km resolution. *Sci. Data* **5**, 180214 (2018).
47. K. Kuusela, The boreal forests: An overview. *Unasylva - No. 170* **43** (1992).
48. F. I. Woodward, *Climate & Plant Distribution* (Cambridge University Press, 1987).
49. D. Siminovitch, Y. Cloutier, Drought and freezing tolerance and adaptation in plants: Some evidence of near equivalences. *Cryobiology* **20**, 487–503 (1983).
50. A. R. Bashforth, W. A. DiMichele, C. F. Eble, W. J. Nelson, Dryland vegetation from the Middle Pennsylvanian of Indiana (Illinois Basin): The dryland biome in glacioeustatic, paleobiogeographic, and paleoecologic context. *J. Paleontol.* **90**, 785–814 (2016).
51. D. K. Brezinski, C. B. Cecil, V. W. Skema, R. Stamm, Late Devonian glacial deposits from the eastern United States signal an end of the mid-Paleozoic warm period. *Palaeogeogr. Palaeoclimatol. Palaeoecol.* **268**, 143–151 (2008).
52. J. P. Wilson, A. H. Knoll, A physiologically explicit morphospace for tracheid-based water transport in modern and extinct seed plants. *Paleobiology* **36**, 335–355 (2010).
53. J. Pittermann, J. S. Sperry, J. K. Wheeler, U. G. Hacke, E. H. Sikkema, Mechanical reinforcement of tracheids compromises the hydraulic efficiency of conifer xylem. *Plant Cell Environ.* **29**, 1618–1628 (2006).
54. J. Pittermann, J. S. Sperry, Analysis of freeze-thaw embolism in conifers. The interaction between cavitation pressure and tracheid size. *Plant Physiol.* **140**, 374–382 (2006).
55. S. D. Davis, J. S. Sperry, U. G. Hacke, The relationship between xylem conduit diameter and cavitation caused by freezing. *Am. J. Bot.* **86**, 1367–1372 (1999).
56. S. Yang, M. T. Tyree, A theoretical model of hydraulic conductivity recovery from embolism with comparison to experimental data on Acer saccharum. *Plant Cell Environ.* **15**, 633–643 (1992).

57. J. Pittermann, J. Sperry, Tracheid diameter is the key trait determining the extent of freezing-induced embolism in conifers. *Tree Physiol.* **23**, 907–914 (2003).
58. C. R. Brodersen, A. J. McElrone, Maintenance of xylem network transport capacity: A review of embolism repair in vascular plants. *Front Plant Sci* **4**, 108 (2013).
59. W. A. DiMichele, R. A. Gastaldo, H. W. Pfefferkorn, Plant biodiversity partitioning in the late carboniferous and early Permian and its implications for ecosystem assembly. *Proc. Calif. Acad. Sci.* **4**, 19 (2005).
60. E. P. Plumstead, The habit of growth of glossopteridae. *Trans. Geol. Soc. S. Afr.* **61**, 81–96 (1958).
61. E. L. Taylor, P. E. Ryberg, Tree growth at polar latitudes based on fossil tree ring analysis. *Palaeogeogr. Palaeoclimatol. Palaeoecol.* **255**, 246–264 (2007).
62. L. Luthardt, R. Rößler, J. W. Schneider, Tree-ring analysis elucidating palaeoenvironmental effects captured in an in situ fossil forest—The last 80 years within an early Permian ecosystem. *Palaeogeogr. Palaeoclimatol. Palaeoecol.* **487**, 278–295 (2017).
63. S. DeWitt, B. Kelly, M. Araiza, P. E. Ryberg, Growth habit indicators from Permian Antarctic glossopterids. *Rev. Palaeobot. Palynol.* **248**, 34–40 (2018).
64. G. T. Creber, W. G. Chaloner, Influence of environmental factors on the wood structure of living and fossil trees. *Bot. Rev.* **50**, 357–448 (1984).
65. H. J. Falcon-Lang, F. Kurzawe, S. G. Lucas, A Late Pennsylvanian coniferopsid forest in growth position, near Socorro, New Mexico, U.S.A.: Tree systematics and palaeoclimatic significance. *Rev. Palaeobot. Palynol.* **225**, 67–83 (2016).
66. J. P. Wilson *et al*., Carboniferous plant physiology breaks the mold. *New Phytol.* **227**, 667–679 (2020).
67. C. Husby, Biology and functional ecology of equisetum with emphasis on the giant horsetails. *Bot. Rev.* **79**, 147–177 (2013).
68. G. W. Rothwell, H. Sanders, S. E. Wyatt, S. Lev-Yadun, A fossil record for growth regulation: The role of auxin in wood evolution[1]. *Ann. Mo. Bot. Gard.* **95**, 121–134 (2008).
69. R. T. Schott, D. Voigt, A. Roth-Nebelsick, Extracellular ice management in the frost hardy horsetail Equisetum hyemale L. *Flora* **234**, 207–214 (2017).
70. F. Shati, S. Prakash, H. Norouzi, R. Blake, Assessment of differences between near-surface air and soil temperatures for reliable detection of high-latitude freeze and thaw states. *Cold Reg. Sci. Technol.* **145**, 86–92 (2018).
71. R. A. Stockey, The Araucariaceae: An evolutionary perspective. *Rev. Palaeobot. Palynol.* **37**, 133–154 (1982).
72. G. W. Stull, W. A. DiMichele, H. J. Falcon-Lang, W. J. Nelson, S. Elrick, Palaeoecology of Macroneuropteris scheuchzeri, and its implications for resolving the paradox of 'xeromorphic' plants in Pennsylvanian wetlands. *Palaeogeogr. Palaeoclimatol. Palaeoecol.* **331–332**, 162–176 (2012).
73. V. L. Harms, G. A. Leisman, The anatomy and morphology of certain cordaites leaves. *J. Paleontol.* **35**, 1041–1064 (1961).
74. L. Kappen, F. Valladares, "Opportunistic growth and desiccation tolerance: The ecological success of poikilohydrous autotrophs" in *Functional Plant Ecology*, F. I. Pugnaire, F. Valladares, Eds. (CRC Press, ed. 2, 2007), pp. 7–66.
75. M. C. F. Proctor, Z. Tuba, Poikilohydry and homoihydry: Antithesis or spectrum of possibilities? *New Phytol.* **156**, 327–349 (2002).
76. G. Goldstein, F. Meinzer, Influence of insulating dead leaves and low temperatures on water balance in an Andean giant rosette plant. *Plant Cell Environ.* **6**, 649–656 (1983).
77. F. Meinzer, G. Goldstein, Some consequences of leaf pubescence in the Andean giant rosette plant Espeletia timotensis. *Ecology* **66**, 512–520 (1985).
78. E. Wohl, "Hydrology and discharge" in *Large Rivers: Geomorphology and Management*, A. Gupta, Ed. (John Wiley & Sons, Ltd, 2007), pp. 29–44.
79. T. J. Algeo, Terrestrial-marine teleconnections in the Devonian: Links between the evolution of land plants, weathering processes, and marine anoxic events. *Philos. Trans. R. Soc. Lond. B Biol. Sci.* **353**, 113 (1998).
80. M. A. Maslin, G. E. A. Swann, "Isotopes in marine sediments" in *Isotopes in Palaeoenvironmental Research*, M. J. Leng, Ed. (Kluwer Academic Publishers, 2006), pp. 227–290.
81. S. I. Macarewich, C. J. Poulsen, I. P. Montañez, Simulation of oxygen isotopes and circulation in a late Carboniferous epicontinental sea with implications for proxy records. *Earth Planet. Sci. Lett.* **559**, 116770 (2021).
82. S. E. Godsey, J. W. Kirchner, D. W. Clow, Concentration-discharge relationships reflect chemostatic characteristics of US catchments. *Hydrol. Processes* **23**, 1844–1864 (2009).
83. D. E. Horton, C. J. Poulsen, D. Pollard, Orbital and CO_2 forcing of late Paleozoic continental ice sheets. *Geophys. Res. Lett.* **34**, L19708 (2007).
84. M. A. Torres, A. J. West, G. Li, Sulphide oxidation and carbonate dissolution as a source of CO2 over geological timescales. *Nature* **507**, 346–349 (2014).
85. F. Jahra, Y. Kawahara, F. Hasegawa, T. Yamamoto, "Effects of floodplain vegetation on flow resistance and large horizontal vortices" in *Proceedings of the 10th International Conference on Hydroscience & Engineering*, (ICHE, 2012).
86. D. M. Lawrence *et al*., The community land model version 5: Description of new features, benchmarking, and impact of forcing uncertainty. *J. Adv. Model. Earth Syst.* **11**, 4245–4287 (2019).
87. M. A. White, P. E. Thornton, S. W. Running, R. R. Nemani, Parameterization and sensitivity analysis of the BIOME-BGC terrestrial ecosystem model: Net primary production controls. *Earth Interact.* **4**, 1–85 (2000).
88. J. S. Golinkoff, *Estimation and Modeling of Forest Attributes Across Large Spatial Scales Using BiomeBGC, High-Resolution Imagery, LiDAR Data, and Inventory Data* (University of Montana, 2013).
89. M. T. van Wijk, M. Williams, G. R. Shaver, Tight coupling between leaf area index and foliage N content in arctic plant communities. *Oecologia* **142**, 421–427 (2005).
90. J. D. White, N. A. Scott, Specific leaf area and nitrogen distribution in New Zealand forests: Species independently respond to intercepted light. *For. Ecol. Manage.* **226**, 319–329 (2006).
91. G. S. Campbell, J. M. Norman, *An Introduction to Environmental Biophysics* (Springer, 1998).
92. T. J. Brodribb, T. S. Feild, G. J. Jordan, Leaf maximum photosynthetic rate and venation are linked by hydraulics. *Plant Physiol.* **144**, 1890–1898 (2007).
93. D. E. Horton, C. J. Poulsen, D. Pollard, Influence of high-latitude vegetation feedbacks on late Palaeozoic glacial cycles. *Nat. Geosci.* **3**, 572–577 (2010).
94. D. E. Horton, C. J. Poulsen, Paradox of late Paleozoic glacioeustasy. *Geology* **37**, 715–718 (2009).
95. F. W. Murray, On the computation of saturation vapor pressure. *J. Appl. Meteorol.* **6**, 203–204 (1967).
96. A. J. Krause *et al*., Stepwise oxygenation of the Paleozoic atmosphere. *Nat. Commun.* **9**, 4081 (2018).
97. I. P. Martini, Ed., *Late Glacial and Postglacial Environmental Changes: Quaternary, Carboniferous-Permian, and Proterozoic* (Oxford University Press, 1997).
98. R. E. Dunn, C. A. E. Strömberg, R. H. Madden, M. J. Kohn, A. A. Carlini, Linked canopy, climate, and faunal change in the Cenozoic of Patagonia. *Science* **347**, 258–261 (2015).
99. C. W. Runyan, P. D'Odorico, D. Lawrence, Physical and biological feedbacks of deforestation. *Rev. Geophys.* **50**, RG4006 (2012).
100. D. P. Lowry, C. J. Poulsen, D. E. Horton, T. H. Torsvik, D. Pollard, Thresholds for Paleozoic ice sheet initiation. *Geology* **42**, 627–630 (2014).
101. S. J. Koenig, R. M. DeConto, D. Pollard, Pliocene Model Intercomparison Project Experiment 1: Implementation strategy and mid-Pliocene global climatology using GENESIS v3.0 GCM. *Geosci. Model Dev.* **5**, 73–85 (2012).
102. G. A. Meehl *et al*., Climate change projections in CESM1(CAM5) compared to CCSM4. *J. Clim.* **26**, 6287–6308 (2013).
103. D. J. Beerling, A. C. Terry, C. Hopwood, C. P. Osborne, Feeling the cold: Atmospheric CO2 enrichment and the frost sensitivity of terrestrial plant foliage. *Palaeogeogr. Palaeoclimatol. Palaeoecol.* **182**, 3–13 (2002).
104. F. Rada, G. Goldstein, A. Azocar, F. Meinzer, Freezing avoidance in Andean giant rosette plants. *Plant Cell Environ.* **8**, 501–507 (1985).
105. W. J. Matthaeus, Command line utilities for performing experiments with *BGC family models: bgc_utils. GitHub. https://github.com/wjmatthaeus/bgc_utils. Deposited 13 April 2021.
106. J. D. White, Model code for "A Process-Based Ecosystem Model (Paleo-BGC) to Simulate the Dynamic Response of Late Carboniferous Plants to Elevated O2 And Aridification". GitHub. https://github.com/josephdwhite/paleo-bgc. Deposited 20 July 2020.
107. W. J. Matthaeus, bgcutils: Serial version. *Zenodo*. https://doi.org/10.5281/zenodo.4686065. Deposited 14 April 2021.
108. W. J. Matthaeus, Data for "Freeze tolerance influenced forest cover and hydrology during the Pennsylvanian". *Dryad*. https://doi.org/10.5061/dryad.qnk98sfgj. Deposited 21 September 2021.